Deep Learning-based Nonlinearity Compensation for Ghost Target Suppression in PMCW Radar Systems

Hyunbin Kim, Soyoon Park, and Seongwook Lee
Department of Electrical and Electronics Engineering
College of ICT Engineering, Chung-Ang University
Seoul, Republic of Korea
{bin000722, thdbs0711, seongwooklee}@cau.ac.kr

***Abstract*—This study proposes a deep-learning-based restoration method that suppresses ghost targets generated by hardware nonlinearity in a phase-modulated continuous-wave (PMCW) radar system. In a PMCW radar system that uses m-sequences, nonlinearity produces cross-terms from signal components with different delays, and the cyclic-shift property of the m-sequence causes these cross-terms to appear as ghost targets in the range–Doppler (RD) map. To address this problem, we propose a restoration method based on a two-dimensional residual network architecture. The proposed method suppresses ghost targets in an RD map caused by hardware nonlinearity, so that the output RD map contains only the actual targets. The performance of the method is evaluated under various signal-to-noise ratio (SNR) levels, and the results show that the method provides consistent restoration performance. The peak signal-to-noise ratio and the signal-to-clutter ratio increase by approximately 14.9 dB and 2.5 dB, respectively, at an SNR of 10 dB. These improvements confirm that the proposed method effectively suppresses ghost targets.**

***Index Terms*—deep neural network, ghost target suppression, nonlinearity, phase-modulated continuous-wave radar.**

I. Introduction

In next-generation radar applications, the demand for high sensing accuracy is rapidly increasing due to the need for reliable target detection and environmental perception [1]. Phase-modulated continuous-wave (PMCW) radar systems support high sensing accuracy using phase-coded waveforms and signal processing based on correlation operations [2]. In particular, PMCW radar systems commonly use binary sequences such as almost perfect sequences (APS), Legendre sequences, and m-sequences, which provide low sidelobes in correlation outputs. This property leads to improved target detection performance. However, APS can be generated only for specific sequence lengths [3]. Legendre sequences also have restricted applicability because their sequence length must be a prime number [4]. In comparison, m-sequences can generate long sequences easily through a linear feedback shift register [5]. For this reason, m-sequences are widely used in PMCW radar systems.

A practical PMCW radar system contains several analog components such as a power amplifier, a mixer, and an analog filter, which have nonlinear characteristics [6]. This nonlinearity distorts the range–Doppler (RD) map, and the distortion pattern depends on the type of binary sequence used in the PMCW radar system. With APS and Legendre sequences, the RD map mainly suffers from increased sidelobes in the presence of hardware nonlinearity [7]. Meanwhile, when an m-sequence is used, ghost targets appear in the RD map, and these ghost targets degrade target-detection performance [8]. To address this issue, a method based on code diversity has been proposed [9]. This approach transmits different sequences across consecutive repetitions so that ghost targets appear at different locations in each repetition. As a result, these ghost targets are attenuated during Doppler processing by applying a discrete Fourier transform (DFT) along the slow-time dimension. However, to maintain the periodicity of the transmitted signal, code diversity requires additional transmissions before switching to a new sequence, which increases system overhead.

In this study, we propose a deep-learning-based method for PMCW radar systems using m-sequences to suppresses ghost targets in RD maps caused by nonlinearity. In contrast to conventional approaches, the proposed method operates at a post-processing stage and does not require modifications to the transmitted sequence or waveform structure. As a result, the proposed method can be directly applied to PMCW radar systems that use m-sequences. The network is trained with RD maps that contain ghost targets as inputs and the corresponding ideal RD maps without ghost targets as ground-truth. Through this training process, the network learns to reconstruct a clean RD map from a distorted one. This enables the model to suppress nonlinear artifacts effectively and preserve the information of actual targets. As a result, the proposed method produces RD maps that are more suitable for accurate target detection.

II. PMCW Radar System and Nonlinearity

A. PMCW Signal Model

In a PMCW radar system, the transmitted signal is generated by modulating the phase of the carrier according to a binary chip sequence using binary phase shift keying modulation. The phase corresponding to each chip is defined as $\phi[n] \in \{0, \pi\}$.

The transmitter sends the same sequence N_s times within one frame. The baseband transmit signal can be expressed as

$$s(t) = \sum_{m=0}^{N_s-1} \sum_{n=0}^{N-1} \exp(j\phi[n])\, p(t - nT_c - mT_s), \quad (1)$$

where n is the fast-time index, m is the slow-time index, and $p(t)$ is a unit rectangular pulse that is equal to 1 for $0 \le t < T_c$ and equal to 0 otherwise. The chip duration and the sequence duration are denoted by T_c and T_s, respectively, where $T_s = NT_c$. The transmit signal is obtained by upconverting the baseband signal to the carrier frequency f_c and is expressed as

$$x(t) = s(t)e^{j2\pi f_c t}. \quad (2)$$

The radio frequency (RF) signal reflected from a single target can be expressed as

$$y_{\mathrm{RF}}(t) = \beta x(t - \tau)e^{j2\pi f_d t}, \quad (3)$$

where β is the complex reflection coefficient of the target, f_d is the Doppler frequency, and τ is the round-trip delay. When the distance and the velocity of the target are R and v, the Doppler frequency and the round-trip delay are given by

$$f_d = \frac{2v}{\lambda} \quad (4)$$

and

$$\tau = \frac{2(R + vt)}{c}, \quad (5)$$

where λ is the wavelength and c is the speed of light. The receiver multiplies the received signal by a local oscillator (LO) signal $e^{-j2\pi f_c t}$ to perform down-conversion. The output of the mixer is filtered by a lowpass filter (LPF) to remove high-frequency components, and the resulting baseband signal can be expressed as

$$y(t) = y_{\mathrm{RF}}(t)e^{-j2\pi f_c t}. \quad (6)$$

When the sampling frequency of the analog-to-digital converter (ADC) is $\frac{1}{T_c}$, the discrete-time received signal can be expressed as

$$y[n, m] = y(nT_c + mT_s). \quad (7)$$

The overall block diagram of the PMCW radar system is shown in Fig. 1.

The range profile is obtained by correlating the received signal reflected from the target with cyclically shifted versions of the transmit sequence, as given by

$$C[k, m] = \sum_{n=0}^{N-1} x^*[\mathrm{mod}(n - k, N)]\, y[n, m]. \quad (8)$$

where k, $(\cdot)^*$, and $\mathrm{mod}(a, N)$ denote the delay index, the complex conjugate, and the modulo operation that returns the remainder of a divided by N, respectively. The range of the target is obtained from the delay index that maximizes the correlation output. Velocity estimation is performed by applying the DFT along the slow-time axis, and the RD map for Doppler bin l can be expressed as

$$D[k, l] = \sum_{m=0}^{M-1} C[k, m] \exp\left(-2\pi j \frac{ml}{M}\right). \quad (9)$$

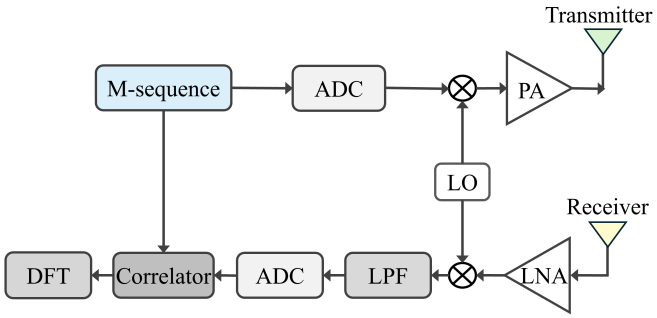

Fig. 1. Overall block diagram of the PMCW radar system.

B. Hardware Nonlinearity in PMCW Radar Systems

The transmit and receive process of a PMCW radar system includes several analog components such as a power amplifier (PA), a mixer, a low-noise amplifier (LNA), and an LPF [10]. These components do not exhibit ideal linear behavior, and such nonlinearity introduces distortion into the radar signal. In this study, we use a simple polynomial model to represent the generalized nonlinearity of the hardware. The input signal of the nonlinear model is denoted by $r(t)$, and the corresponding output of the model is given by

$$u(t) = a_1 r(t) + a_2 |r(t)|^2 + a_3 |r(t)|^3, \quad (10)$$

where a_1, a_2, and a_3 are complex coefficients that represent the linear and nonlinear characteristics of the system. The first term represents the output of an ideal linear system. The second and third terms correspond to nonlinear components of the polynomial model and generate distortion in the received signal. When signal components with different delays pass through a nonlinear system, products among the delayed signal components are generated, including cross-terms. These cross-terms appear as distortion in the RD map.

III. Impact of Nonlinearity in PMCW Radar Systems

The impact of nonlinearity in a PMCW radar system depends on the type of binary sequence used. For APS and Legendre sequences, the cross-terms induced by nonlinearity appear without regularity [7]. In this case, nonlinearity appears as increased sidelobes in the RD map. For m-sequences, the product of two delayed versions of the sequence results in another cyclically shifted sequence [5]. If we denote the m-sequence by $b[n] \in \{-1, +1\}$, this property can be expressed as

$$b[n]\, b[n - \tau] = b[n - \tau']. \quad (11)$$

Therefore, when the received signal passes through a nonlinear system, signal components with different cyclic shifts are generated. These components appear as ghost targets at different ranges after the correlation process.

When a single target is present and the LPF does not introduce delayed replicas, the LPF output can be expressed as $y_{\mathrm{LPF}}(t) = y(t)$. In this case, the nonlinear system operates on a single delay component and does not generate coupling terms between different delays. When the nonlinearity introduced by the second-order term is considered, the output includes a term $|y(t)|^2$. This term does not contain delay information and therefore does not produce ghost targets. In a practical PMCW radar system, however, the residual response of the LPF may create multiple delayed replicas of a single target. Let us assume that the signal filtered by the LPF can be expressed as

$$y_{\mathrm{LPF}}(t) = h_0 y(t) + h_1 y(t-1) + h_2 y(t-2). \tag{12}$$

When this signal passes through a nonlinear system, the second-order term becomes

$$\begin{aligned} |y_{\mathrm{LPF}}(t)|^2 = {} & h_0^2|y(t)|^2 + h_1^2|y(t-1)|^2 + h_2^2|y(t-2)|^2 \\ & + 2h_0h_1 y(t)y(t-1) + 2h_0h_2 y(t)y(t-2) \\ & + 2h_1h_2 y(t-1)y(t-2). \end{aligned} \tag{13}$$

The expression includes terms with a single delay component, such as $h_0^2|y(t)|^2$ and $h_1^2|y(t-1)|^2$, and these terms do not generate ghost targets. In contrast, cross-terms such as $2h_0h_1y(t)y(t-1)$ represent the product of signal components that have different delays, and these cross-terms result in ghost targets. When the RD map is obtained from a signal that has passed through the second-order nonlinear term, this component does not retain any Doppler information. Fig. 2 shows RD maps obtained from received signals generated with nonlinear terms of different orders and different numbers of targets. In Fig. 2 (a), when only the nonlinearity introduced by the second-order term is present, ghost targets appear at the zero-Doppler bin. In contrast, the third-order term multiplies the original signal again, and the Doppler information is preserved. As a result, the ghost targets appear at different ranges, and their velocities are identical to those of the actual target, as shown in Fig. 2 (b).

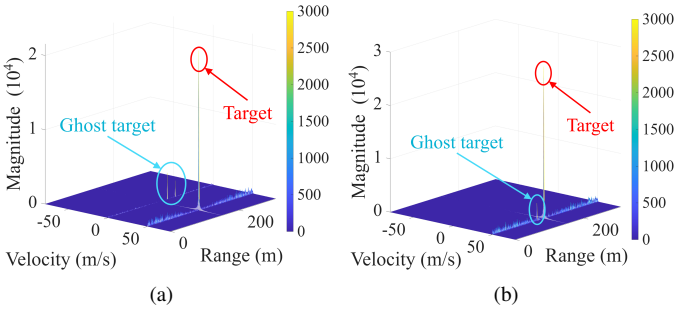

Fig. 2. RD maps in a single-target scenario: (a) with nonlinearity induced by the second-order term and (b) with nonlinearity induced by the third-order term.

When more than one target exists, the received signal contains the reflections from the targets as well as delayed replicas generated by the filter response. When this signal passes through the nonlinear system, products among these delayed components are formed, resulting in more cross-terms than in the single-target case. These cross-terms appear as ghost targets at various Doppler bins in the resulting RD map due to the property of m-sequences, and their locations do not correspond to those of the actual targets.

IV. Proposed Method

In this study, we propose a deep-learning-based restoration method for PMCW radar systems using m-sequences. The proposed method takes as input an RD map generated under nonlinear conditions, which contains both actual targets and ghost targets, and restores the RD map by suppressing ghost targets. The network is trained using corresponding ideal RD maps generated under the same target configuration but without nonlinear distortion. When nonlinear distortion is present, ghost targets appear at distinct range bins determined by the cyclic-shift property of the m-sequence. Since these patterns of ghost-target appearance are consistently observed in the RD maps and are closely related to the order of the nonlinear terms, the proposed model learns to effectively distinguish ghost targets from actual targets.

To this end, we adopt a two-dimensional (2D) residual network (ResNet) architecture. Because each RD map is complex-valued, the network receives a two-channel input consisting of the real and imaginary parts of the RD map. The network is designed to reconstruct a two-channel RD map with the same spatial resolution as the input. This design preserves the residual learning structure of ResNet and enables the model to learn spatial patterns that distinguish ghost targets from actual targets. The first layer consists of a 7×7 convolutional (Conv) layer followed by group normalization (GN) and a rectified linear unit (ReLU), increasing the number of channels from 2 to 16. The network then consists of four stages, and each stage contains two bottleneck blocks. Each bottleneck block consists of a 1×1 Conv layer, a 3×3 Conv layer, and a 1×1 Conv layer, and these three layers perform channel reduction, spatial feature extraction, and channel expansion, respectively. We apply GN so that the model can learn stably under various signal-to-noise ratio (SNR) conditions, and we use ReLU as the activation function. When the number of input and output channels differs, a shortcut consisting of a 1×1 Conv layer and GN is used. This shortcut forms a residual connection that enables the essential features of the RD map to propagate through deep layers without degradation. Each stage uses internal bottleneck channels of 16, 32, 64, and 128. At the final 1×1 Conv layer, the number of channels is expanded by a factor of four, resulting in output channel sizes of 64, 128, 256, and 512. All stages use a stride of one so that the spatial resolution of the RD map is preserved throughout the entire network. This design allows the model to learn the spatial structure of ghost targets without any loss of resolution. Finally, a 3×3 Conv layer reduces the number of channels to

2, and the network produces a restored two-channel RD map. Fig. 3 shows the complete architecture of the ResNet-based network.

V. Performance Evaluation

A. Simulation Setup

The performance of the proposed method was evaluated using RD maps generated based on the simulation parameters listed in Table I. Using the same simulation settings, a total of 500 RD maps were generated for each SNR level. Among them, 80% of the RD maps were used for training and the remaining 20% were used for testing. The SNR level was varied to evaluate the restoration performance of the proposed method under different noise conditions. The coefficients

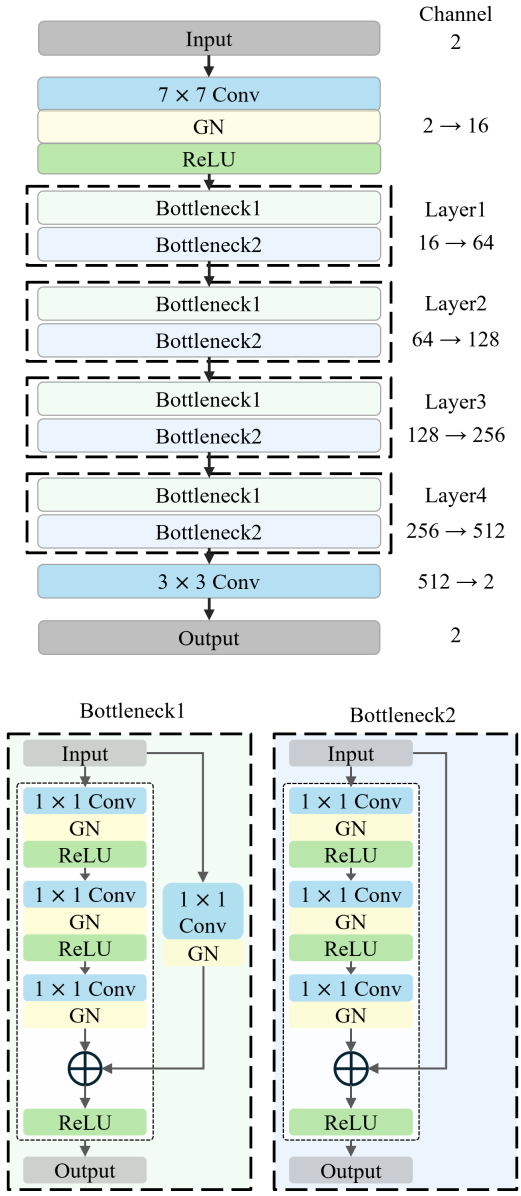

Fig. 3. Structure of the proposed 2D ResNet.

TABLE I
Simulation Parameters Used In The PMCW Radar System

Parameter	Value
Center frequency, f_c	77 GHz
Speed of light, c	3×10^8 m/s
Bandwidth, B	0.5 GHz
Number of chips, N	511
Number of pulses N_s	256
Range of the target	10 m $\sim$ 140 m
Velocity of the target	-150 m/s $\sim +150$ m/s
SNR	0 dB, 5 dB, 10 dB, 15 dB, 20 dB
Filter coefficients, g_1, g_2, g_3	$0 \sim 1$
Linear coefficient, a_1	1
Nonlinear coefficients, a_2, a_3	$0.1 \sim 0.5$

(g_0, g_1, g_2) describing the LPF response were selected from the range $[0, 1]$ and arranged in descending order such that $g_0 > g_1 > g_2$. The coefficients were then scaled so that their sum equals one. During network training, the mean squared error (MSE) was used as the loss function, and the network was trained using the adaptive moment estimation optimizer for 100 epochs.

Fig. 4 shows the restoration results of the proposed method in a two-target scenario. The targets are located at $(49.87\ \text{m},\ -137.44\ \text{m/s})$ and $(42.10\ \text{m},\ -287.48\ \text{m/s})$. Fig. 4 (a) shows the input RD map generated under nonlinear distortion, and Fig. 4 (b) shows the corresponding ground-truth RD map obtained from an ideal system. Fig. 4 (c) shows the restored RD map produced by the proposed ResNet. In Fig. 4 (c), the ghost targets observed in the input are effectively suppressed, while the peaks corresponding to the actual targets are preserved. These results confirm that the proposed method effectively suppresses various ghost targets caused by nonlinearity while preserving the actual target information.

B. Performance Analysis

The performance of the proposed method was evaluated using the peak signal-to-noise ratio (PSNR) and the signal-to-clutter ratio (SCR). The input PSNR, denoted as PSNR_{in}, measures the similarity between the input RD map and the ground-truth RD map. It is defined as

$$\text{PSNR}_{\text{in}} = 10 \log_{10} \left(\frac{D_{\max}^2}{\text{MSE}(D_{\text{in}}, D_{\text{gt}})} \right). \tag{14}$$

Here, $D_{\max}$ denotes the maximum value of the ground-truth RD map, i.e., $D_{\max} = \max(D_{\text{gt}})$. The term $\text{MSE}(D_{\text{in}}, D_{\text{gt}})$ represents the MSE between the input RD map D_{in} and the ground-truth RD map D_{gt}. Similarly, the output PSNR, denoted as PSNR_{out}, measures the similarity between the restored RD map and the ground-truth RD map. It is defined as

$$\text{PSNR}_{\text{out}} = 10 \log_{10} \left(\frac{D_{\max}^2}{\text{MSE}(D_{\text{out}}, D_{\text{gt}})} \right), \tag{15}$$

After applying the proposed method, the PSNR is significantly improved, with PSNR_{out} ranging from 53.01 dB to 64.14 dB across all SNR levels. These results demonstrate that the restored RD maps achieve a high similarity to the

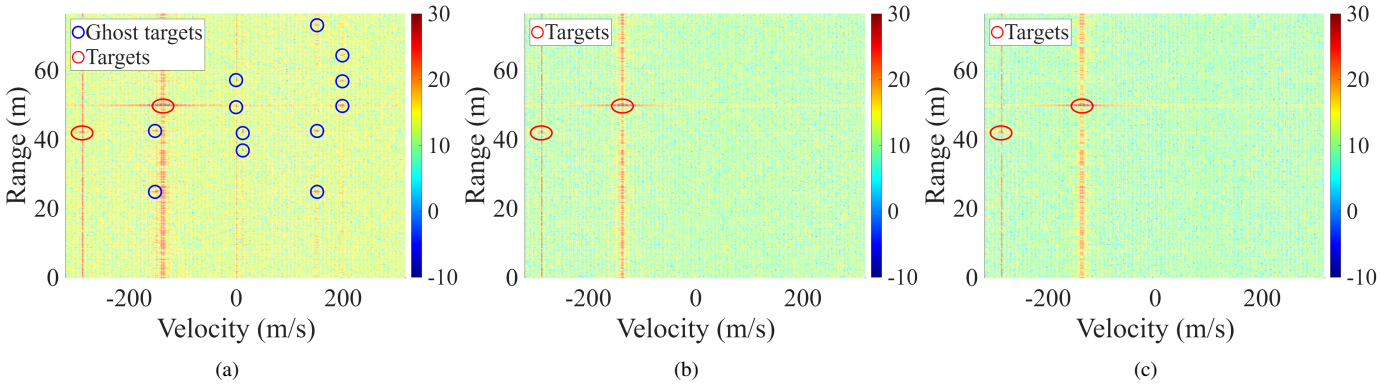

Fig. 4. Ghost-target suppression results on RD maps: (a) an input RD map containing ghost targets, (b) a ground-truth RD map obtained from an ideal system, and (c) a restored RD map produced by the proposed method.

ground-truth RD maps. As a representative example, at an input SNR of 10 dB, the proposed method improves the PSNR from 46.50 dB to 61.37 dB, corresponding to a gain of 14.87 dB. This improvement indicates that the proposed method effectively suppresses ghost components caused by nonlinearity. where D_{out} denotes the restored RD map. All RD maps were normalized by $D_{\max}$ prior to PSNR computation. Fig. 5 (a) presents the PSNR results for different input SNR levels. The input RD maps show PSNR_{in} values ranging from 39.84 dB to 47.20 dB.

Another evaluation metric, SCR reflects how effectively ghost components are suppressed and is defined as

$$\text{SCR} = 10\log_{10}\left(\frac{P_{\text{target}}}{P_{\text{clutter}}}\right), \tag{16}$$

where P_{target} and P_{clutter} denote the power of the target region and the background region, respectively. Because the number and locations of ghost targets depend on the number of actual targets and the order of the nonlinear terms, SCR is an appropriate evaluation metric that can be computed without explicitly separating ghost targets from the background. Fig. 5 (b) shows the SCR improvement for different input SNR levels, and the improvement ranges from 2.39 dB at an SNR of 0 dB to 2.60 dB at an SNR of 20 dB. These results indicate that ghost targets are suppressed across all SNR levels. For an input SNR of 10 dB, the SCR improvement is 2.50 dB, confirming that the proposed method effectively reduces ghost targets.

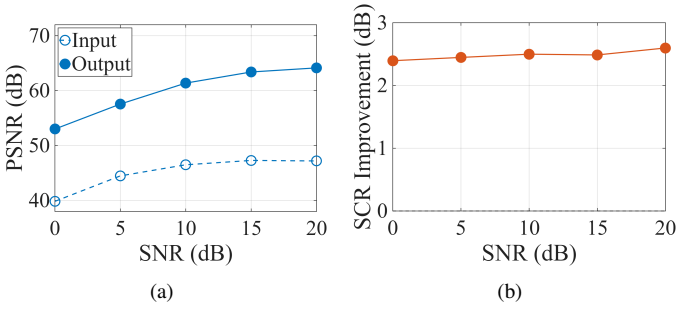

Fig. 5. Performance improvement under different SNR levels: (a) PSNR improvement and (b) SCR improvement.

VI. Conclusion

This study proposed a restoration method to address the ghost target problem caused by nonlinearity in a PMCW radar system. The proposed method used a 2D ResNet architecture that received an RD map containing ghost targets and restored the map while preserving only the actual targets. The network was designed to learn the spatial patterns of ghost targets that repeatedly appeared due to nonlinearity. The performance of the proposed method was evaluated using an RD map dataset with different numbers of targets and various SNR levels. At an SNR of 10 dB, the PSNR increased from 46.5 dB for the input RD map to 61.4 dB after applying the proposed method, corresponding to an improvement of approximately 14.9 dB. The SCR increased by 2.50 dB, confirming that the proposed method effectively suppressed ghost targets. These results demonstrate that the proposed method provides stable RD map restoration in the presence of hardware nonlinearity. Consequently, the proposed method enhances the reliability of range and velocity estimation in PMCW radar systems.

Acknowledgment

This work was supported by the National Research Foundation of Korea (NRF) grant funded by the Korea government (MSIT) (No. RS-2025-16068888).

References

[1] M. Kahlert, T. Fei, Y. Wang, C. Tebruegge, and M. Gardill, "Unified model and survey on modulation schemes for next-generation automotive radar systems", *Remote Sensing*, vol. 17, no. 8, pp. 1–43, March 2025.

[2] C. Park, J. -H. Park, T. Jeong, J. Joung, and S. Lee, "Efficient frame structure design of PMCW radar based on golay sequence in 802.11ad preamble," *IEEE Internet of Things Journal*, vol. 12, no. 24, pp. 53177–53189, December 2025.

[3] J. Wolfmann, "Almost perfect autocorrelation sequences," *IEEE Transactions on Information Theory*, vol. 38, no. 4, pp. 1412–1418, July 1992.

[4] J. M. Baden, "Legendre sequences for periodic non-coherent pulse compression," *IET Radar, Sonar Navigation*, vol. 10, no. 1, pp. 225—226, January 2016.

[5] S. Orth and H. Klingbeil, "Maximum length binary sequences and spectral power distribution of periodic signals," *EURASIP Journal on Advances in Signal Processing*, vol. 2024, no. 80, pp. 1–23, July 2024.
[6] D. Eustice, C. Baylis, L. Cohen, and R. J. Marks, "Effects of power amplifier nonlinearities on the radar ambiguity function," *2015 IEEE Radar Conference (RadarCon)*, Arlington, USA, May 2015, pp. 1725–1729.
[7] U. Ahmad, D. Guermandi, A. Medra, W. Van Thillo, and A. Bourdoux, "Impact of even and odd order non-linearity on PMCW radars," *2016 IEEE Radar Conference (RadarConf)*, Philadelphia, USA, May 2016, pp. 1–5.
[8] R. Lin, Y. Chen, and J. Li, "On properties of periodic binary sequences in the presence of system non-linearities," *IEEE Transactions on Signal Processing*, vol. 70, pp. 3400–3413, June 2022.
[9] M. Bauduin and A. Bourdoux, "Code diversity for range sidelobe attenuation in PMCW and OFDM radars," *2021 IEEE Radar Conference (RadarConf21)*, Atlanta, USA, pp. 1–5, May 2021.
[10] M. Lübke, Y. Su, and N. Franchi, "Evaluating RF hardware characteristics for automotive JCRS systems based on PMCW-CDMA at 77GHz," *IEEE Access*, vol. 11, pp. 28565–28584, March 2023.